Artificial Intelligence in Geosciences 4 (2023) 128–136

Contents lists available at ScienceDirect

Artificial Intelligence in Geosciences

journal homepage: www.keaipublishing.com/en/journals/artificial-intelligence-in-geosciences

Original research articles

Automated stratigraphic correlation of well logs using Attention Based Dense Network

Yang Yang [a], Jingyu Wang [b], Zhuo Li [a], Naihao Liu [a,*], Rongchang Liu [c], Jinghuai Gao [a], Tao Wei [d]

[a] School of Information and Communications Engineering, Xi'an Jiaotong University, Xi'an, Shaanxi 710049, China
[b] School of Software Engineering, Xi'an Jiaotong University, Xi'an, Shaanxi 710049, China
[c] PetroChina Research Institute of Petroleum Exploration and Development (RIPED), CNPC, Beijing 100083, China
[d] Research Institute of Exploration and Development, Yumen Oilfield Company, CNPC, Jiuquan, Gansu 735019, China

ARTICLE INFO

Keywords:
Automated stratigraphic correlation
Attention Based Dense Network
Densely connected convolutional network
Squeeze and Excitation Block

ABSTRACT

The stratigraphic correlation of well logs plays an essential role in characterizing subsurface reservoirs. However, it suffers from a small amount of training data and expensive computing time. In this work, we propose the Attention Based Dense Network (ASDNet) for the stratigraphic correlation of well logs. To implement the suggested model, we first employ the attention mechanism to the input well logs, which can effectively generate the weighted well logs to serve for further feature extraction. Subsequently, the DenseNet is utilized to achieve good feature reuse and avoid gradient vanishing. After model training, we employ the ASDNet to the testing data set and evaluate its performance based on the well log data set from Northwest China. Finally, the numerical results demonstrate that the suggested ASDNet provides higher prediction accuracy for automated stratigraphic correlation of well logs than state-of-the-art contrastive UNet and SegNet.

1. Introduction

Establishing the stratigraphic framework is a crucial technology in geological interpretation (Cross and Lessenger, 1988), which is beneficial for reservoir estimation and geologic model building (Fang et al., 2021). Stratigraphic correlation is a widely used approach to provide information regarding stratigraphic and compartmentalization in a reservoir. For the traditional process of seismic interpretation, stratigraphic correlation is often obtained by geological interpreters, which is time-consuming and heavily reliant on the expertise of the interpreters (Tokpanov et al., 2020). To avoid the above problems, automatic stratigraphic correlation approaches have been proposed, employing computational algorithms and statistical methods to analyze stratigraphic data from different locations and determine the relative ages of rock layers or sedimentary deposits. Over the past decades, many automatic stratigraphic correlation approaches have been employed, such as the cross-correlation technique (Southam and Hay, 1978; Mann and Dowell, 1978), dynamic waveform matching technique (Smith and Waterman, 1980; Edwards et al., 2018), dynamic time warping (Wheeler and Hale, 2014; Behdad, 2019) and its improvements (Grant et al., 2018). These approaches mitigate the reliance on geological interpreters. However, they usually introduce several fine-tuning parameters to obtain a precise stratigraphic correlation result, which is important but difficult to select.

Recently, with the rapid development of deep learning (DL), convolutional neural networks (CNNs) have attracted more researchers' attention in seismic signal processing and interpretation (Liu et al., 2021; Dong et al., 2022; Lou et al., 2022a; Liu et al., 2022c), mainly including seismic fault detection, seismic facies analysis, seismic noise reduction, seismic inversion, etc. Generally, CNNs-based approaches are also utilized in stratigraphic correlation. Maniar et al. (2018) proposed to use CNN and multilayer perceptron for semiautomatic stratigraphic correlation. Zhang et al. (2019) suggested a CNN-aided workflow to interpret a large amount of well-log data. Recently, more and more state-of-the-art CNNs models are introduced for stratigraphic division and correlation. For example, SegNet, which is stable to process pixel-based data, has been adapted to correct stratigraphic (Xu et al., 2019; Dai et al., 2021). The Bidirectional Long Short-Term Memory (BiLSTM) and the Inception autoencoder CNN are also applied to interpret the log data and these two models are proved to be effective for the stratigraphic interpretation (Tokpanov et al., 2020). Generally, these DL-based stratigraphic correlation methods is a pixel

* Corresponding author.
E-mail addresses: yang_yang@mail.xjtu.edu.cn (Y. Yang), jingyu_work@163.com (J. Wang), xjtu_lizhuo@stu.xjtu.edu.cn (Z. Li), naihao_liu@mail.xjtu.edu.cn (N. Liu), liurongchang1115@163.com (R. Liu), jhgao@mail.xjtu.edu.cn (J. Gao), 675125007@qq.com (T. Wei).

https://doi.org/10.1016/j.aiig.2023.09.001
Received 7 April 2023; Received in revised form 30 August 2023; Accepted 11 September 2023
Available online 18 September 2023

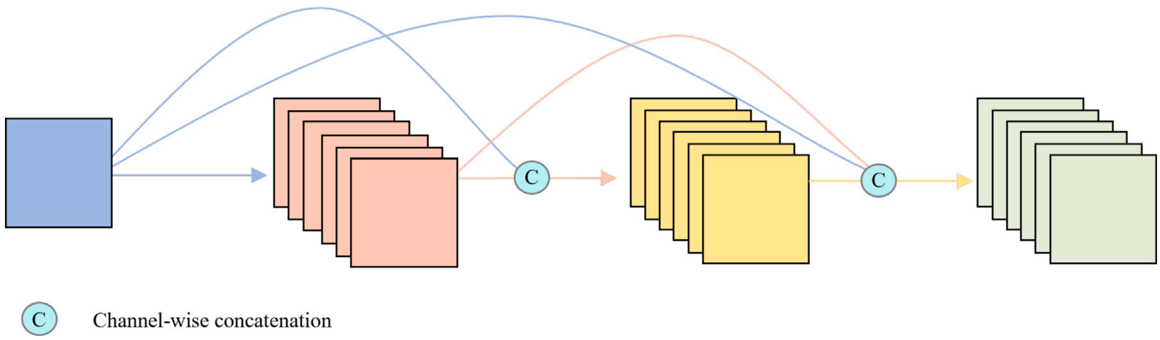

Fig. 1. The simplified architecture of the Dense Block.

classification, which is similar to semantic segmentation. This is the reason that several semantic segmentation-based models are utilized to solve stratigraphic correlation issues (Dai et al., 2021; Wang and Chen, 2023). Except for the model architecture, the loss function is another key factor for the success of a CNN model. There are several excellent loss functions proposed for solving different tasks (Liu et al., 2022b,d; Yang et al., 2022), which have also been applied to address the accurate stratigraphic correlation (Tokpanov et al., 2020; Liu et al., 2022a).

Among these state-of-the-art DL models, the densely connected convolutional network (DenseNet) stands out with its intriguing connectivity pattern, where each layer is connected to all the others within a dense block (Zhu and Newsam, 2017). The DenseNet is more compact and is not easy to overfit. Furthermore, this architecture ensures that each layer directly benefits from supervision by the loss function, thereby facilitating deep supervision. Benefiting from these advantages, the DenseNet has been adopted for addressing different issues, such as medical data analysis (Wang et al., 2019; Zhang et al., 2020a), landslide detection (Cai et al., 2021), image segmentation (Zhang et al., 2023, 2020b), etc. In consideration of these advantages of DenseNet, we suggest a DenseNet-based workflow for automated stratigraphic correlation in this study, termed the Attention Based Dense Network (ASDNet). Since the attention mechanism allows DL models to weigh different parts of the input, which can be useful for interpreting how the model is making its predictions, we introduce the Squeeze and Excitation Block (SEBlock). Certainly, we first take different well logs of a certain well as the multi-channel input of the suggested model. Next, the SEBlock is utilized to calculate self-attention on the input channels, which aim to weigh different well logs. Afterward, the dense blocks are combined with convolutional layers to generate feature maps, which are utilized to get the classification result of the input well. Afterward, to test the effectiveness of the ASDNet, we apply it to the well log data set for the automated stratigraphic correlation, which is located at Ordos Basin, Northwest China.

2. Methodology

2.1. Dense convolutional network

To enhance the performance of convolutional neural networks, deepening the network is frequently proposed and utilized. Recently, He et al. (2016) proposed the Residual Networks (ResNet), which utilizes the identity connections to address the gradient vanishing caused by network depth. Similar to ResNet, the Dense Convolutional Network (DenseNet) is suggested to utilize the dense connection to connect all layers directly with each other (Huang et al., 2019), which contributes to better feature reuse and contains fewer parameters. The Dense Block mainly consists of non-linear transformation and Transition layers. As depicted in Fig. 1, the rectangular blocks indicate both the inputs of each layer and the outputs of previous layers. It is worth noting that we do not draw non-linear transformation and Transition layers in the figure, but instead use arrows to represent them. Specifically, the output of the ith layer can be written as

$$x_i = F_i\left(\left[x_0, x_1, \ldots, x_{i-1}\right]\right), \tag{1}$$

where $\left[x_0, x_1, \ldots, x_{i-1}\right]$ indicates the concatenation of the feature maps computed in the preceding layers. $0, \ldots, i-1$. $F_i(\cdot)$ refers to the non-linear transformation of the ith layer, which can be defined as a combination of the batch normalization (BN), rectified linear unit (ReLU), and 2D convolution (Conv). Moreover, the channel size of x_i is k, which is defined as the growth rate and means each layer in the Dense Block produces k feature maps. The dense connections shown in Eq. (1) make the information flow and gradients easy to propagate while reducing the parameters. However, note that a dense block may generate a staggering amount of feature maps. To solve this problem, the Transition layer is introduced. The Transition layer is used to connect the Dense Block and reduce the channels of feature maps by utilizing a Conv with kernel size 1×1. The above series of non-linear transformations constitute a Dense Block. Note that, in this study, we remove the max pooling operation in the traditional Transition layer to lower the precision loss in downsampling, which would be explained in the following sub-sections.

2.2. Squeeze and excitation block

To investigate the relationship between different channels, Hu et al. (2018) proposed the Squeeze and Excitation Block (SEBlock). The network can recalibrate the features with the aid of the SEBlock, indicating that it can learn to strengthen informative features and weaken redundant ones. As presented in Fig. 2, the SEBlock maps the input X to the refined feature maps $\tilde{X}$, where $X \in \mathbb{R}^{C\times H\times W}$ and $\tilde{X} \in \mathbb{R}^{C\times H\times W}$. Overall, the whole process of the SEBlock can be divided into three parts: the squeeze, excitation, and scale. Given an input X, it first utilizes squeeze operation F_s to produce aggregating feature maps across spatial dimensions, where F_s can be defined as the global average pooling or global max pooling. Next, the squeezed feature maps via a simple gating mechanism F_e can be implemented by two fully-connected (FC) layers, to get the weight of channel dimensions, written as S_c. Finally, the scale operation F_{sc} utilizes the channel-wise multiplication between S_c and X to re-scale the input X to the weighted output $\tilde{X}$.

2.3. ASDNet

Based on the substructures in the previous sub-sections, we propose the Attention Based Dense network (ASDNet) for automated stratigraphic correlation of well logs in this study. Fig. 3 shows the simplified architecture and the corresponding detailed operations of the suggested ASDNet.

Since the well logs of a single well can be regarded as a multi-channel vector, we concatenate the well logs as the input. To make the model simpler and make full use of CNN's characteristics, we reshape

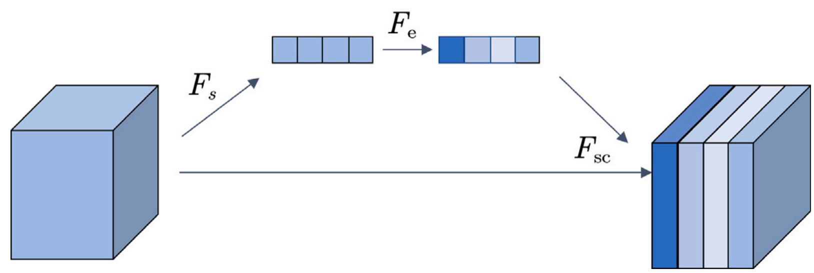

Fig. 2. The simplified architecture of the Squeeze and Excitation Block. F_s, F_e, and F_{sc} indicate the squeeze operation, the simple gating mechanism, and the scale operation, respectively.

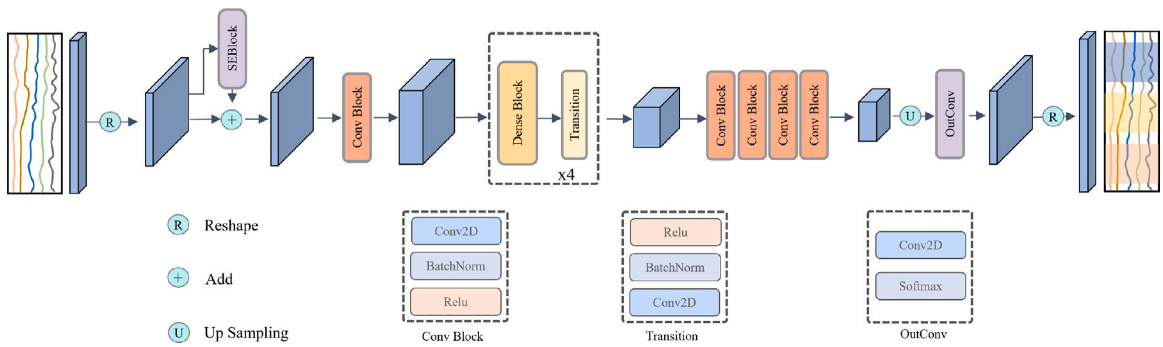

Fig. 3. The simplified architecture of the suggested ASDNet.

the input multi-channel vector into a multi-channel matrix. Afterward, we employ the mentioned SEBlock as a bypass to calculate the refined feature maps of self-attention on the input channels, which aim to weigh different well logs. Then, the refined feature maps are added to the input via a connection-skipping operation. Here, we add a Conv Block shown in Fig. 3 to increase the channel size so that it can be directly applied to the following Dense Blocks. Here, to have a balance between model parameters and computational efficiency, we set four Dense Blocks. The combination of all these modules and the Dense Blocks can generate reduced feature maps with abundant information. Therefore, it should be noted that this part can also be interpreted as an encoder.

The second half of the ASDNet can be regarded as a decoder. It starts with four Conv Blocks to maintain the non-linear transformation while downscaling the channel size of the reduced feature maps generated by the encoder. Afterward, we apply two up-sampling layers followed by the OutConv and reshape operation, which are utilized to map the size of feature maps to the original well log length and get classification results. Based on the above operations, we can get the accurate stratigraphic correlation of corresponding well logs.

3. Numerical results

3.1. Study area and well logs

The study area is located in the Ordos Basin, Northwest of China, indicated by the red ellipse in Fig. 4. This study area is located near the western margin of the North China craton, which is proved to be a low porosity and low permeability reservoir (Wang et al., 2015). Studies have indicated that the Chang 7 member (i.e., the target interval) shows complex and anisotropic stratigraphic characteristics, therefore, it is a difficult task to accurately implement stratigraphic correlation of well logs in this survey.

Fig. 5 presents the well map of the used well logs in this study. There are a total of 176 wells in this seismic survey. Note that the

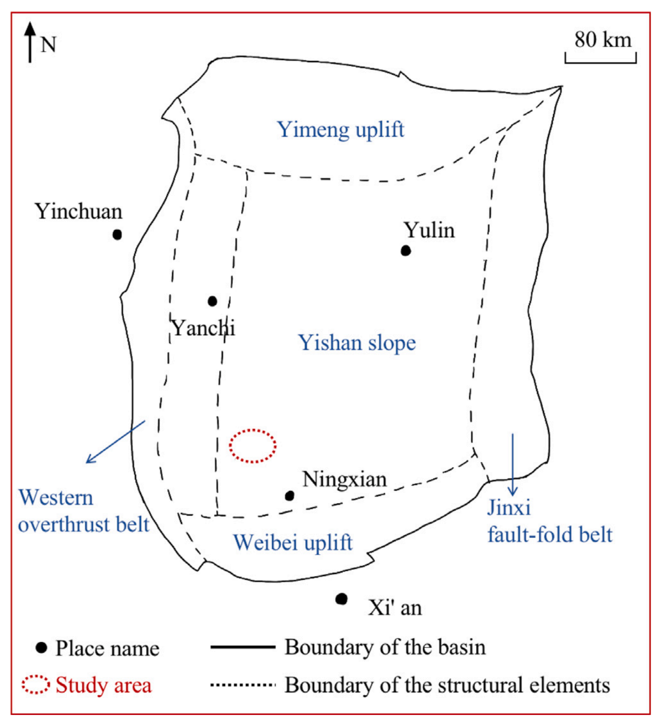

Fig. 4. The study area is located in the northwest of China, indicated by the red ellipse.

red and blue dots present the training and blind test wells, i.e., 88 wells and 88 wells, respectively. Here, the number of training wells is given by experiments. We select borehole diameter (CAL), spontaneous potential (SP), gamma ray (GR), acoustic (AC), and formation resistivity (RT) as the training data in this study. Note that there are several other commonly used well logs, such as density (DEN) and neutron

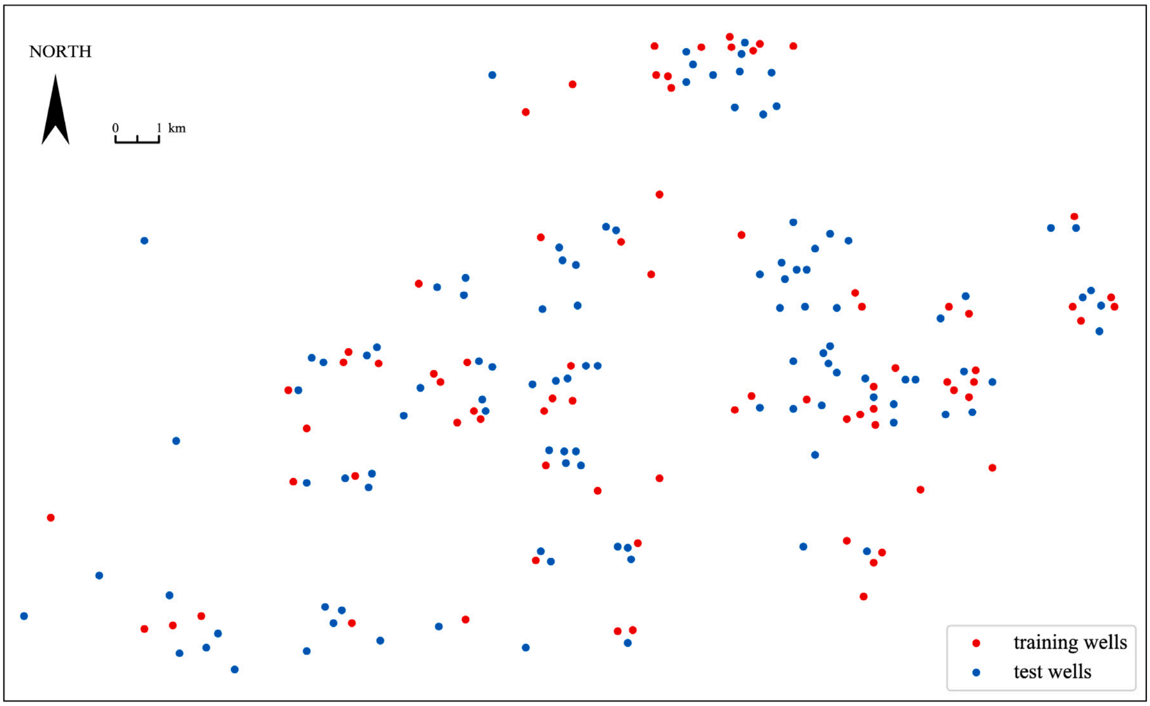

Fig. 5. The well borehole locations at the study area, where the red and blue dots present the training and blind test wells.

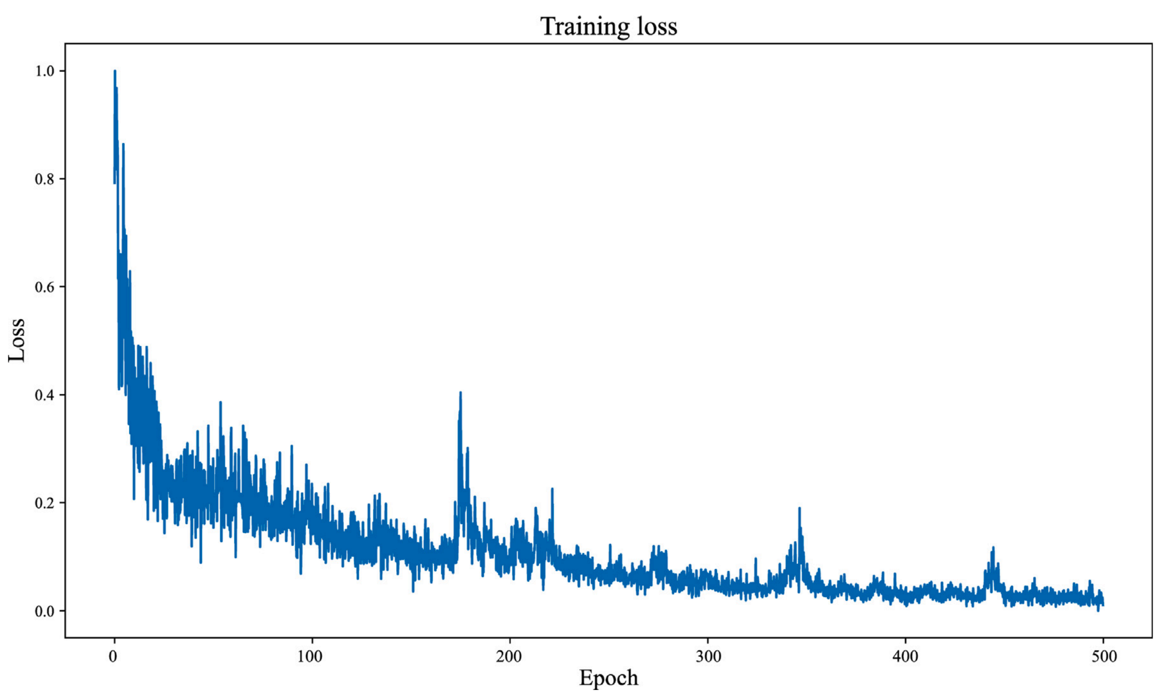

Fig. 6. The training loss curve of ASDNet.

porosity (CNL). Due to the confidentiality agreement, we cannot obtain more kinds of well logs, therefore, we do not implement the ablation study about the sensitive well log selection in this work. It should be noticed that sensitivity analysis of well logs is important for automated stratigraphic correlation with the aid of deep learning.

3.2. Model training

All the DL models used in this study are created using Python 3.7 and the PyTorch deep learning library in version 1.11.0. Moreover, we implement all the computations mentioned above on a server equipped with a 36-core processor, 256 GB RAM, and NVIDIA GTX 3090 (24 GB GPU memory). To balance the training effectiveness and convergence rate, the models are each trained with a batch size of 16 and a maximum of 500 epochs. To be more specific, we use the Adam optimizer with a learning rate of 0.0001 and a weight decay of 0.001. The other hyperparameters of the Adam optimizer are set by default. In addition, the loss function is set as the cross entropy loss in this work.

To train and validate the proposed ASDNet, the wells of the data set are randomly divided into training wells and blind testing wells,

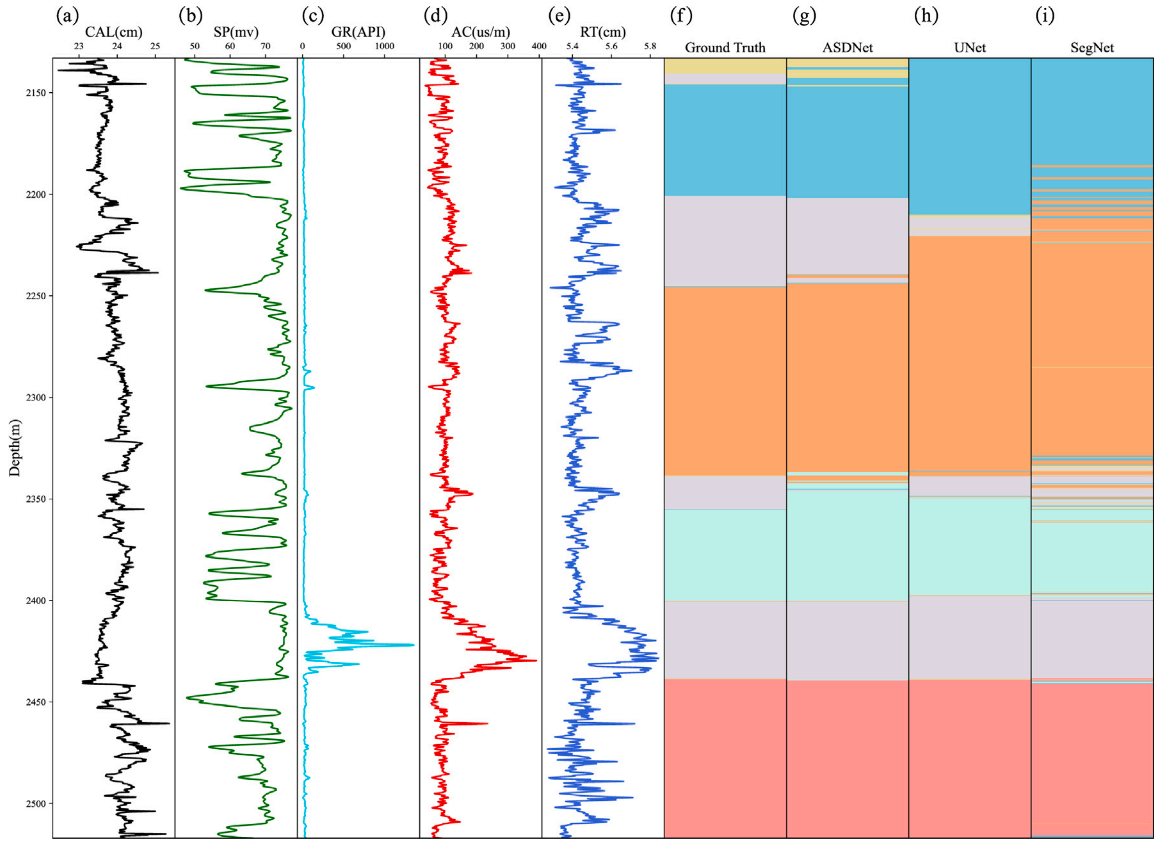

Fig. 7. Well logs and automated stratigraphic correlation at Well 37, (a)–(e) five well logs, (f) ground truth stratigraphic correlation, (g)–(h) automated stratigraphic correlation results calculated using ASDNet, UNet, and SegNet.

Table 1
The confusion matrix of the binary classification results.

		Predicted result	
		Positive	Negative
Ground truth label	Positive	True Positive (TP)	False Negative (FN)
	Negative	False Positive (FP)	True Negative (TN)

indicated in Fig. 5. After the fine-tuning training, the training loss curve of training data is presented by the blue in Fig. 6. To more clearly see how values are changing, we normalize the loss value in Fig. 6. Obviously, the ASDNet is easy to converge and converges at around 400 epochs. After model training, we obtain an accurate and convergent ASDNet.

3.3. Model evaluation

To evaluate the performance of ASDNet, we introduce several evaluation indicators to quantitatively test the effectiveness of the proposed model, including the Accuracy (Acc) and confusion matrix. The Confusion matrix summarizes the data set's entries in the form of a matrix based on the ground truth label and the prediction of the well-trained model. The real value is represented by the row of the matrix, while the predicted value is represented by the column of the matrix. Table 1 denotes the confusion matrix of binary classification results and multi-classification may be deduced by analogy.

3.4. Stratigraphic correlation results

After model training, we apply different models to the blind testing data set for model validation and detailed comparison. We first randomly select Well 37 (W37) to visualize the predicted result of ASDNet. Moreover, to make equitable comparisons, we apply the same well to other deep learning models, including UNet and SegNet. Note that UNet and SegNet are two commonly used semantic segmentation-based DL models, which have also been successfully used for addressing geological issues (Liu et al., 2020; Birnie et al., 2021; Meng et al., 2021; Gupta et al., 2022; Lou et al., 2022b). Therefore, we adopt them as the contrastive methods in this study. It should be noted that the UNet and SegNet utilized in this work are standard implementations, which both contain five layers for encoding and decoding. As indicated in Fig. 7, the input of DL models is composed of five curves, which are respectively (a) CAL, (b)GR, (c) SP, (d) AC, and (e) RT. The prediction results of these deep learning models are shown in Fig. 7(g)–7(i), while the ground truth labels are presented in Fig. 7(f). Comparing these stratigraphic correlation results in Fig. 7, we can easily observe that ASDNet achieves the most precise results, especially for label 1 (straw yellow parts), while SegNet gets the worst results that cannot predict label 1. Moreover, there are too many misinterpreted thin layers in Fig. 7(i). Although the prediction results of ASDNet demonstrate its superiority for automated stratigraphic correlation, its interpretation at stratigraphic boundaries should be further enhanced.

Next, the confusion matrices of Well 37 are computed using (a) ASDNet, (b) UNet, and (c) SegNet and indicated in Fig. 8. Most of confusion values in Fig. 8(a) are larger than those in Fig. 8(b) and 8(c). These confusion matrices quantificationally demonstrate the superiority of the suggested model over UNet and SegNet for automated stratigraphic correlation.

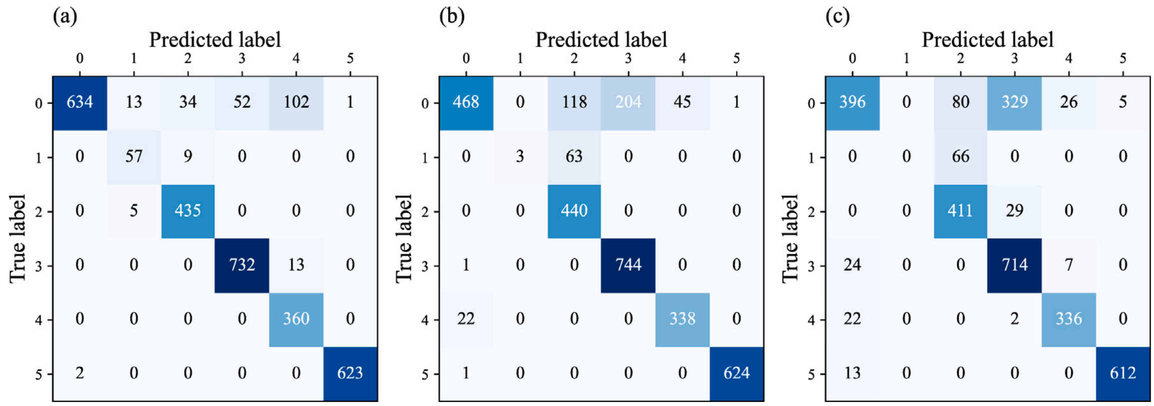

Fig. 8. The confusion matrices of Well 37 computed using (a) ASDNet, (b) UNet, and (c) SegNet.

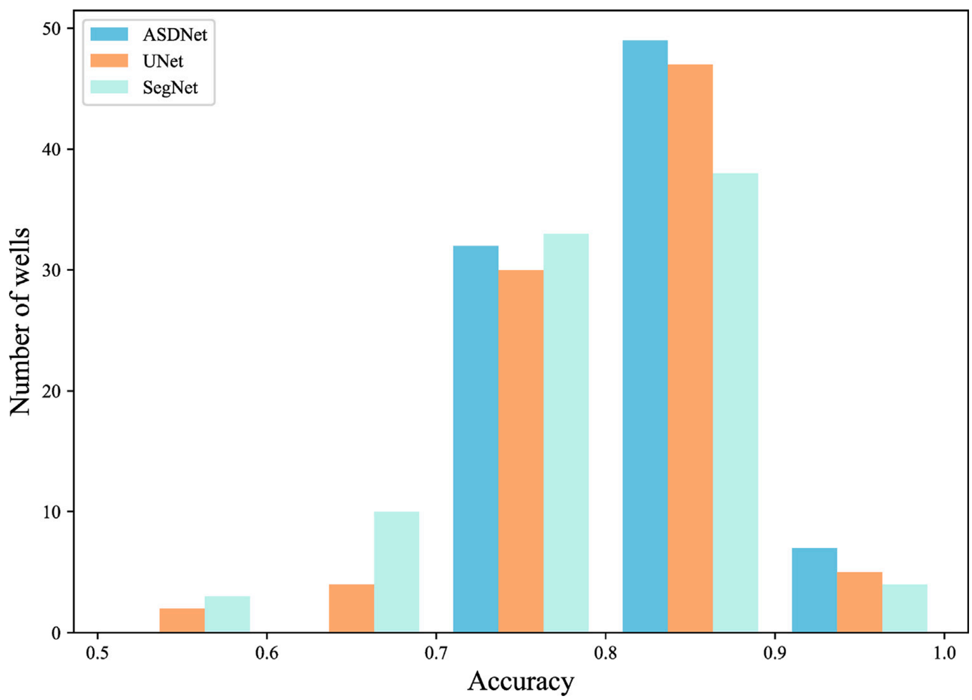

Fig. 9. The accuracy of the total blind test data set computed using different deep learning models.

After the comparisons of W37, we then compare the overall performance for the whole blind testing data set. Fig. 9 shows the accuracy of the total blind test data set computed using different models. The horizontal axis indicates the normalized accuracy, while the vertical axis presents the well numbers. Obviously, the suggested ASDNet provides stratigraphic correlation results of all well boreholes with an accuracy higher than 0.7. Nevertheless, UNet and SegNet show apparently worse results than ASDNet, even resulting in accuracy lower than 0.6. In addition, the average accuracies of the whole blind testing data set are calculated using different models and shown in Table 2. The suggested ASDNet achieves about 3% and 4% accuracy enhancement over UNet and SegNet. These quantitative comparisons in Fig. 9 and Table 2 further prove the availability and stableness of the suggested ASDNet for automated stratigraphic correlation of well logs.

Finally, we present the automated stratigraphic correlation results of multiple wells in Fig. 10, Fig. 11 and Fig. 12, respectively calculated using UNet, SegNet, and ASDNet. The solid and dashed lines indicate the ground truth and predicted stratigraphic correlation results for W20, W42, and W49. Similar to the above discussions, the suggested model apparently provides more accurate stratigraphic correlation results than the other two methods, especially at deep layers.

Table 2
The average accuracy (Acc) calculated using different models.

Model	UNet	SegNet	ASDNet
Acc	0.7944	0.7822	**0.8208**

4. Discussion

Efficiency: Deep learning model inference times have a strong connection with the network architecture. The model's computational complexity and inference speed are directly influenced by the network structure's design and the number of parameters. Since the proposed ASDNet introduces the attention module, the total computing complexity of the proposed model increases. Therefore, we decrease the number

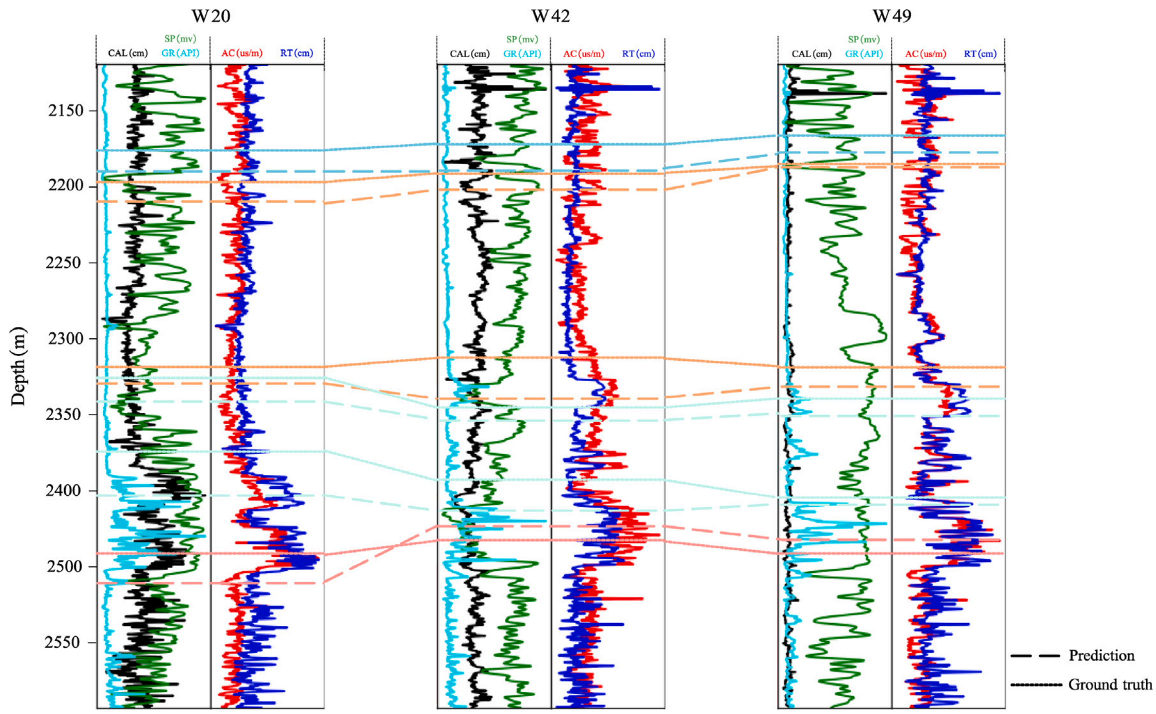

Fig. 10. The stratigraphic correlation results of multiple wells computed using UNet and the stratigraphic correlation results of ground truth. The solid and dashed lines indicate the ground truth and predicted stratigraphic correlation results, respectively.

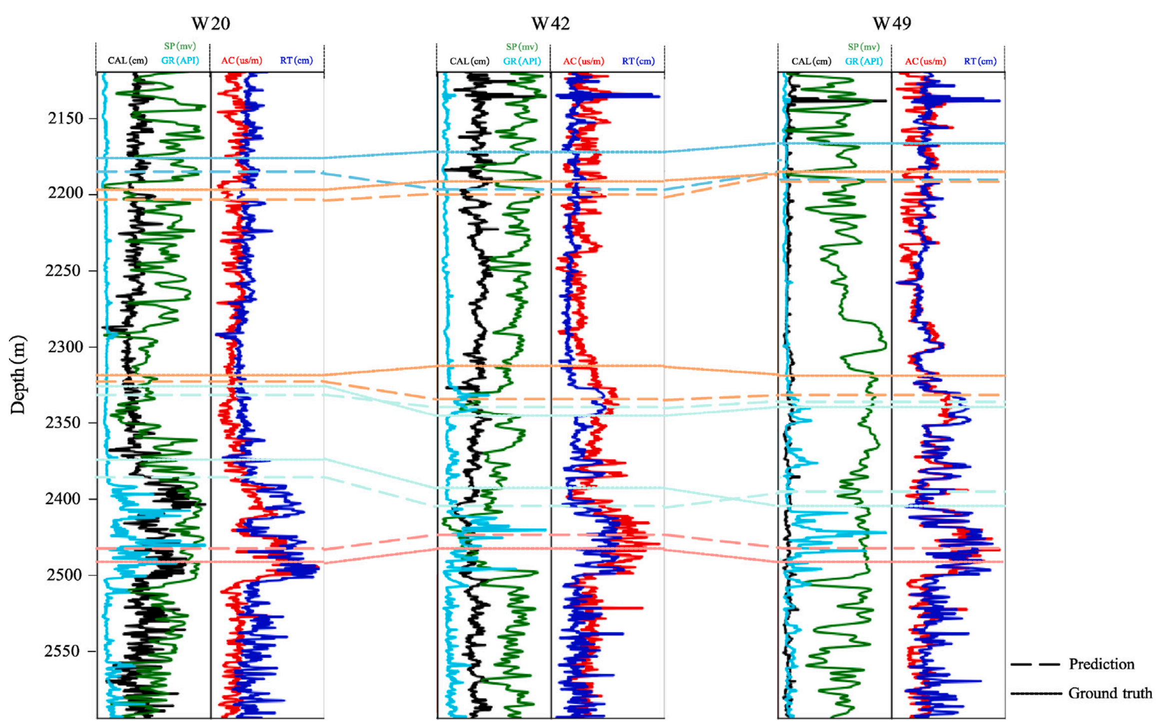

Fig. 11. The stratigraphic correlation results of multiple wells computed using SegNet and the stratigraphic correlation results of ground truth. The solid and dashed lines indicate the ground truth and predicted stratigraphic correlation results, respectively.

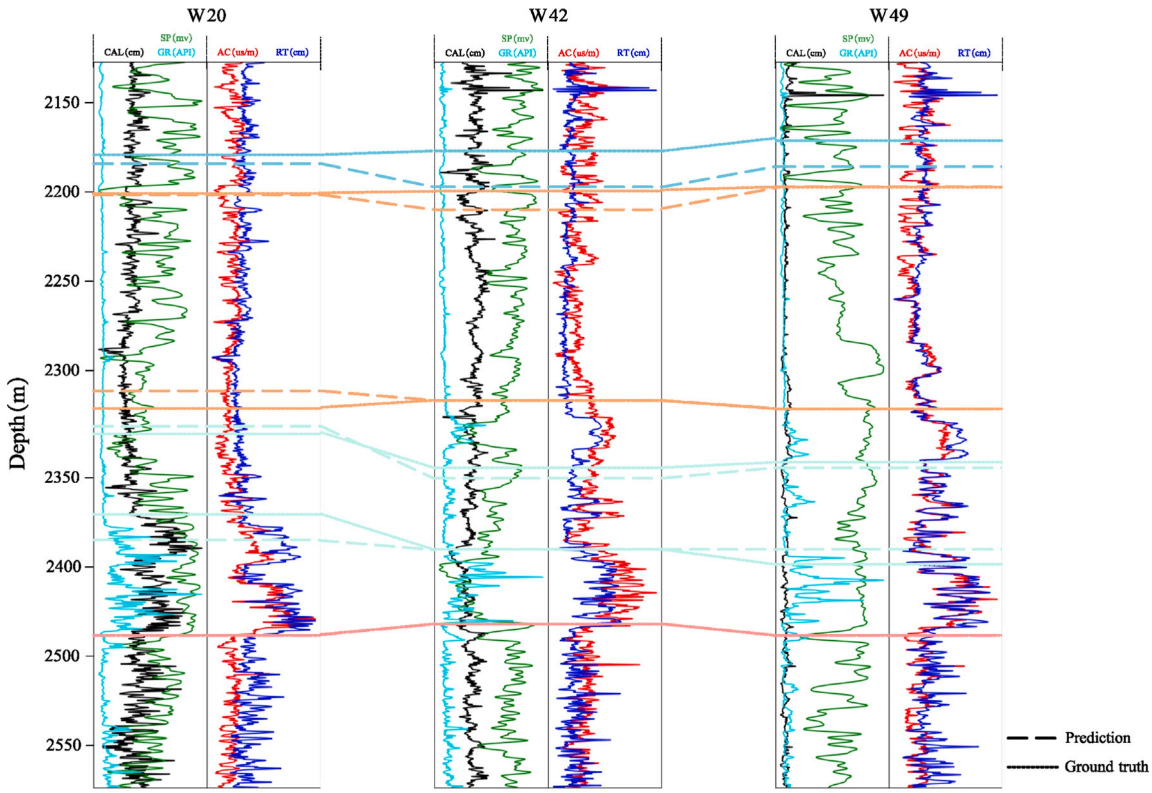

Fig. 12. The stratigraphic correlation results of multiple wells computed using ASDNet and the stratigraphic correlation results of ground truth. The solid and dashed lines indicate the ground truth and predicted stratigraphic correlation results, respectively.

Table 3
The average training times for an epoch over the training data set and the inference times over the testing data set.

Model	UNet	SegNet	ASDNet
Training time (s)	0.721	0.347	0.875
Inference time (s)	0.267	0.112	0.297

of up-sampling operations to lower the computing complexity and information loss. Moreover, we compare the training times and inference time of ASDNet with other methods over the training and testing data set, indicated in Table 3. It can be observed that the proposed ASDNet just slightly increases the computation time compared with UNet.

Limitation: A deep learning model is suggested for implementing automated stratigraphic correlation of well logs. Note that the suggested ASDNet is actually a supervised model, indicating that we need a large number of labeled data as training data and training labels. These training labels are interpreted by experienced interpreters or calculated using traditional methods, which is time-consuming and laborious work. Moreover, the precision of training labels plays an important role in the success of a deep learning model. In future work, we would like to introduce other state-of-the-art tools for determining the confidence intervals of the automated stratigraphic correlation results. Moreover, unsupervised models can also be utilized to solve automated well log correlation issues, such as Gaussian mixture model-based methods.

Future work: As discussed above, the stratigraphic correlation of well logs is regarded as a segmentation task in this study. Therefore, we suggested a segmentation model, i.e., the Attention Based Dense Network (ASDNet), to enhance the performance of stratigraphic correlation. Certainly, the suggested ASDNet can be easily transferred to address other geological segmentation issues, such as horizon picking and fault interpretation.

5. Conclusion

In this study, we suggest an ASDNet model for automated stratigraphic correlation of well logs, with the aid of the Dense Convolutional Network (DenseNet) and the Squeeze and Excitation Block (SEBlock). Specifically, the introduction of SEBlock and DenseNet can successfully explore the relationship of different well logs while facilitating meaningful feature reuse. The numerical examples prove that the SEBlock can adequately model channel-wise feature dependencies. Moreover, the DenseNet exhibits robust performance in extracting features from the appropriately weighted well logs. The qualitative and quantitative experiments finally demonstrate the superiority of the proposed ASDNet, which is superior to state-of-the-art semantic segmentation models, i.e., UNet and SegNet.

Declaration of competing interest

The authors declare that they have no known competing financial interests or personal relationships that could have appeared to influence the work reported in this paper.

Acknowledgments

This research was supported by the Key Research and Development Program of Shaanxi, China under Grant 2023-YBGY-076, the Fundamental Research Funds for the Central Universities, China under Grant XZY012022086 and the China Postdoctoral Science Foundation Project under Grant 2022M712509. The authors would like to thank the Research Institute of Exploration and Development, Yumen Oilfield Company (CNPC) for providing the license for the data set used in this study.

References

Behdad, A., 2019. A step toward the practical stratigraphic automatic correlation of well logs using continuous wavelet transform and dynamic time warping technique. J. Appl. Geophys. 167, 26–32.

Birnie, C., Ravasi, M., Liu, S., Alkhalifah, T., 2021. The potential of self-supervised networks for random noise suppression in seismic data. Artif. Intell. Geosci. 2, 47–59.

Cai, H., Chen, T., Niu, R., Plaza, A., 2021. Landslide detection using densely connected convolutional networks and environmental conditions. IEEE J. Sel. Top. Appl. Earth Obs. Remote Sens. 14, 5235–5247.

Cross, T.A., Lessenger, M.A., 1988. Seismic stratigraphy. Annu. Rev. Earth Planetary Sci. 16 (1), 319–354.

Dai, Y., Huang, X., Liu, H., Yang, H., Wei, G., Lu, N., Han, Z., Song, H., 2021. Stratigraphic automatic correlation using SegNet semantic segmentation model. In: SEG/AAPG/SEPM First International Meeting for Applied Geoscience & Energy. OnePetro.

Dong, X., Lin, J., Lu, S., Huang, X., Wang, H., Li, Y., 2022. Seismic shot gather denoising by using a supervised-deep-learning method with weak dependence on real noise data: A solution to the lack of real noise data. Surv. Geophys. 43 (5), 1363–1394.

Edwards, J., Lallier, F., Caumon, G., Carpentier, C., 2018. Uncertainty management in stratigraphic well correlation and stratigraphic architectures: A training-based method. Comput. Geosci. 111, 1–17.

Fang, H., Lou, Y., Zhang, B., Xu, H., Lu, M., 2021. Mimicking the process of manual sequence stratigraphy well correlation. Interpretation 9 (3), T667–T684.

Grant, C.W., Bashore, W.M., Compton, S., 2018. Rapid reservoir modeling with automated tops correlation. In: Unconventional Resources Technology Conference, Houston, Texas, 23-25 July 2018. Society of Exploration Geophysicists, American Association of Petroleum …, pp. 4004–4019.

Gupta, T., Zwartjes, P., Bamba, U., Ghosal, K., Gupta, D.K., 2022. Near-surface velocity estimation using shear-waves and deep-learning with a U-net trained on synthetic data. Artif. Intell. Geosci. 3, 209–224.

He, K., Zhang, X., Ren, S., Sun, J., 2016. Deep residual learning for image recognition. In: Proceedings of the IEEE Conference on Computer Vision and Pattern Recognition. pp. 770–778.

Hu, J., Shen, L., Sun, G., 2018. Squeeze-and-excitation networks. In: Proceedings of the IEEE Conference on Computer Vision and Pattern Recognition. pp. 7132–7141.

Huang, G., Liu, Z., Pleiss, G., Van Der Maaten, L., Weinberger, K.Q., 2019. Convolutional networks with dense connectivity. IEEE Trans. Pattern Anal. Mach. Intell. 44 (12), 8704–8716.

Liu, N., He, T., Tian, Y., Wu, B., Gao, J., Xu, Z., 2020. Common-azimuth seismic data fault analysis using residual UNet. Interpretation 8 (3), SM25–SM37.

Liu, N., Huang, T., Gao, J., Xu, Z., Wang, D., Li, F., 2021. Quantum-enhanced deep learning-based lithology interpretation from well logs. IEEE Trans. Geosci. Remote Sens. 60, 1–13.

Liu, N., Li, Z., Chen, J., Liu, Y., Wu, H., Gao, J., Zhou, X., 2022a. The edge-guided FPN model for automatic stratigraphic correlation of well logs. J. Pet. Sci. Eng. 218, 110985.

Liu, N., Wang, J., Gao, J., Chang, S., Lou, Y., 2022b. Similarity-informed self-learning and its application on seismic image denoising. IEEE Trans. Geosci. Remote Sens. 60, 1–13.

Liu, N., Wang, J., Gao, J., Yu, K., Lou, Y., Pu, Y., Chang, S., 2022c. NS2NS: Self-learning for seismic image denoising. IEEE Trans. Geosci. Remote Sens. 60, 1–11. http://dx.doi.org/10.1109/TGRS.2022.3217289.

Liu, N., Wu, L., Wang, J., Wu, H., Gao, J., Wang, D., 2022d. Seismic data reconstruction via wavelet-based residual deep learning. IEEE Trans. Geosci. Remote Sens. 60, 1–13.

Lou, Y., Li, S., Li, S., Liu, N., Zhang, B., 2022a. Seismic volumetric dip estimation via multichannel deep learning model. IEEE Trans. Geosci. Remote Sens. 60, 1–14.

Lou, Y., Wu, L., Liu, L., Yu, K., Liu, N., Wang, Z., Wang, W., 2022b. Irregularly sampled seismic data interpolation via wavelet-based convolutional block attention deep learning. Artif. Intell. Geosci..

Maniar, H., Ryali, S., Kulkarni, M.S., Abubakar, A., 2018. Machine-learning methods in geoscience. In: 2018 SEG International Exposition and Annual Meeting. OnePetro.

Mann, C.J., Dowell, Jr., T.P., 1978. Quantitative lithostratigraphic correlation of subsurface sequences. Comput. Geosci. 4 (3), 295–306.

Meng, F., Fan, Q., Li, Y., 2021. Self-supervised learning for seismic data reconstruction and denoising. IEEE Geosci. Remote Sens. Lett. 19, 1–5.

Smith, T.F., Waterman, M.S., 1980. New stratigraphic correlation techniques. J. Geol. 88 (4), 451–457.

Southam, J.R., Hay, W.W., 1978. Correlation of stratigraphic sections by continuous variables. Comput. Geosci. 4 (3), 257–260.

Tokpanov, Y., Smith, J., Ma, Z., Deng, L., Benhallam, W., Salehi, A., Zhai, X., Darabi, H., Castineira, D., 2020. Deep-learning-based automated stratigraphic correlation. In: SPE Annual Technical Conference and Exhibition. OnePetro.

Wang, D., Chen, G., 2023. Intelligent seismic stratigraphic modeling using temporal convolutional network. Comput. Geosci. 171, 105294.

Wang, Z., Gao, J., Wang, D., Wei, Q., 2015. 3D seismic attributes for a tight gas sand reservoir characterization of the eastern Sulige gas field, Ordos Basin, China. Geophysics 80 (2), B35–B43.

Wang, H., Shen, Y., Wang, S., Xiao, T., Deng, L., Wang, X., Zhao, X., 2019. Ensemble of 3D densely connected convolutional network for diagnosis of mild cognitive impairment and Alzheimer's disease. Neurocomputing 333, 145–156.

Wheeler, L., Hale, D., 2014. Simultaneous correlation of multiple well logs. In: 2014 SEG Annual Meeting. OnePetro.

Xu, Z., Liu, Y., Zhou, X., He, H., Zhang, B., Wu, H., Gao, J., 2019. An experiment in automatic stratigraphic correlation using convolutional neural networks. Petrol. Sci. Bull. 1, 1–10.

Yang, Y., Lei, Y., Liu, N., Wang, Z., Gao, J., Ding, J., 2022. SparseTFNet: A physically informed autoencoder for sparse time–frequency analysis of seismic data. IEEE Trans. Geosci. Remote Sens. 60, 1–12.

Zhang, B., Liu, Y., Zhou, X., Xu, Z., 2019. Accelerate well correlation with deep learning. Explorer, August 18–19.

Zhang, T., Luo, Y.m., Li, P., Liu, P.z., Du, Y.z., Sun, P., Dong, B., Xue, H., 2020a. Cervical precancerous lesions classification using pre-trained densely connected convolutional networks with colposcopy images. Biomed. Signal Process. Control 55, 101566.

Zhang, Z., Wu, C., Coleman, S., Kerr, D., 2020b. DENSE-INception U-net for medical image segmentation. Comput. Methods Programs Biomed. 192, 105395.

Zhang, J., Zhang, Y., Jin, Y., Xu, J., Xu, X., 2023. Mdu-net: Multi-scale densely connected u-net for biomedical image segmentation. Health Inf. Sci. Syst. 11 (1), 13.

Zhu, Y., Newsam, S., 2017. Densenet for dense flow. In: 2017 IEEE International Conference on Image Processing. ICIP, IEEE, pp. 790–794.